

NEANDC ( OR ) - 156 " U "

INDC ( SWT ) - 15 / L

PROGRESS REPORT TO NEANDC  
FROM SWITZERLAND

May 1981

F. Widder

Swiss Federal Institute for Reactor Research  
Würenlingen

~~NOT FOR PUBLICATION~~

## PREFACE

This document contains information of a preliminary or private nature and must be used with discretion. Its contents may not be quoted, abstracted, reproduced, transmitted to libraries or societies or formally referred to without the explicit permission of the originator.

## CONTENTS

I.	Institut de Physique, Université de Neuchâtel	1
II.	Physik-Institut der Universität Zürich	3
III.	Laboratorium für Kernphysik der ETH Zürich	10
IV.	Eidg. Institut für Reaktorforschung, Würenlingen	12

I. Institut de Physique, Université de Neuchâtel

1. The n-d elastic differential cross section at 2.01 MeV

J. Weber

The method used for this measurement has already been described elsewhere [1], [2]. The preliminary results are shown in the figure. The angular domain of measurement is limited by electronic thresholds. It is to be noted that the data analysis method produces the coefficients of a polynomial function representing the cross section in the center of mass. It is this function that is depicted in the figure. In ref. [1] one can find a description of a possible way of extracting, from such a function, a statistical set of data that could be used in ERA analysis for example.

New measurements are in progress at the same neutron energy in order to increase the statistics and therefore the accuracy of our results especially at large angles.

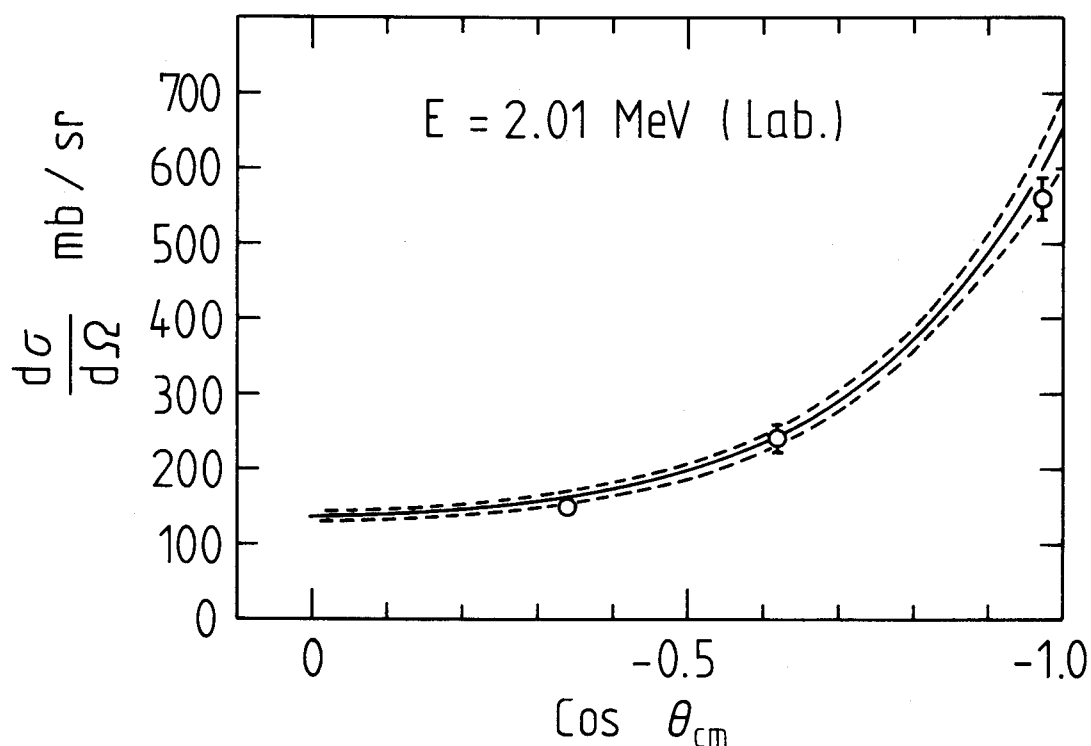


Figure : n-d elastic differential cross section.

— present results as explained in the text.

---- confidence limits (one S.D.).  $\bigcirc$  Elwyn and Lane's data at 1.95 MeV, Phys. Rev. 128 (1962) 779.

### References

- {1} P. Chatelain, Y. Onel and J. Weber, Nucl. Phys. A319 (1979) 71.
- {2} P. Chatelain, Y. Onel and J. Weber, Nucl. Inst. Meth. 151 (1978) 519.

### 2. The ERA analysis of the n-d cross section and depolarization data

R. Viennet and J. Weber

Our ERA code {1} is currently used to analyse our depolarization {2} and cross section {3} data. As expected from theoretical arguments, the depolarization data are of utmost importance in determining the 2S and especially the 2P partial waves contributions.

A paper presenting the results of this analysis is being prepared.

### References

- {1} R. Viennet and J. Weber, Progress Report to NEANDC from Switzerland, June 1980, p. 2.
- {2} D. Bovet et al., Progress Report to NEANDC from Switzerland, June 1979, p. 3.
- {3} P. Chatelain, Y. Onel and J. Weber, Nucl. Phys. A319 (1979) 71.

II. Physik-Institut der Universität Zürich

---

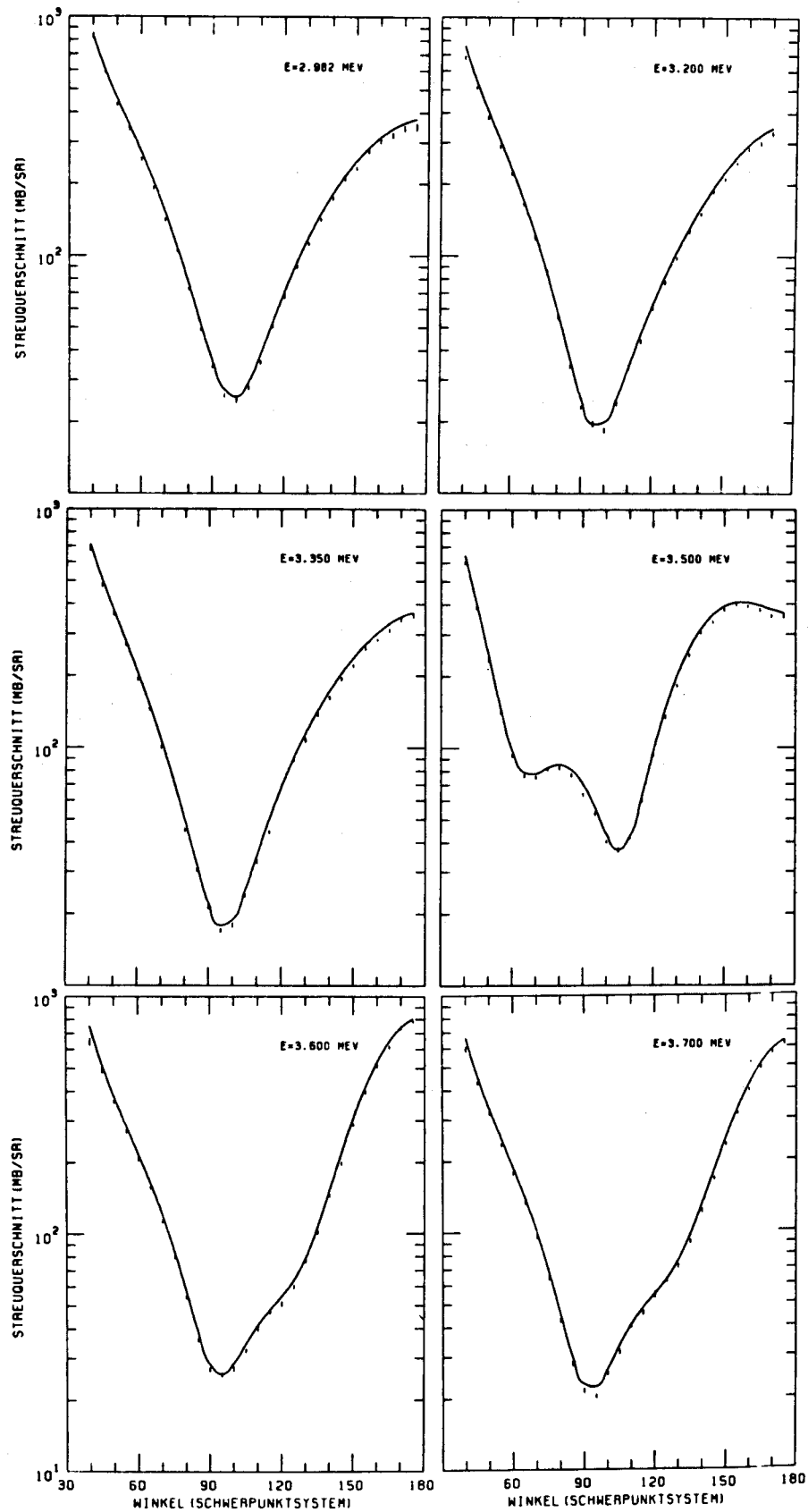
1.  ${}^6\text{Li}$ - $\alpha$ -scattering between 3 and 4 MeV

M. Berta, R. Pixley, V. Meyer

The measurements which we reported in the 1979 progress report have been evaluated and are being published {1}. In the meantime we have pursued our investigation to higher energies. Our particular aim was to definitely establish the spin and parity of a pronounced resonance at  $E_\alpha = 3.5$  MeV. Accurate angular distributions were measured up to 4 MeV and a phase fit (solid lines in the figure) was obtained. While all other phases were rather smoothly through the resonance the  $l = 3$ ,  $J = 4$  phase rises from approx.  $0^\circ$  at 3.20 MeV to  $170^\circ$  at 3.70 MeV thus showing a typical resonant behaviour. The spin and parity of the 3.5 MeV resonance ( $E_x = 6.56$  MeV in  ${}^{10}\text{B}$ ) are therefore  $J^\pi = 4^-$  in accord with tentative assignments of Refs. {2} and {3}, but contrary to Ref. {4} who assumed a positive parity for this state.

References

- {1} M. Berta et al., Nucl. Phys. A357 (1981)
- {2} V. Meyer et al., Nucl. Phys. A101 (1967) 321
- {3} F. Young et al., Nucl. Phys. A176 (1971) 289
- {4} A.J. Sierk et al., Nucl. Phys. A210 (1973) 341



Angular distributions of  $\alpha$ -particles scattered on  ${}^6\text{Li}$

2. Study of preequilibrium-emission in  $(\vec{p}, \alpha_x)$ - reactions

H.H. Müller et al., R. Wagner\* et al.

In the past few years there has been a growing interest in nuclear reactions, like  $A(p, \alpha \dots)X$ . Preequilibrium reaction-models have been applied to describe the angular distribution of the  $\alpha$ -particles and the high energy region of the continuum spectra. In such calculations it is assumed that the projectile interacts stepwise with the target nucleus, each step producing a more complex configuration, where an increasing number of nucleons share the available excitation energy. At each stage there is some probability for the emission of the complex particle. From experiments using polarized particles in the entrance channel, one can hope to get a direct information about the time-development and relaxation of the nuclear system. If, in the pre-equilibrium region, more or less direct contributions dominate the emission, one would expect a strong analyzing power that could reach deep into the continuum. The measurement of the angular distribution of the analyzing power could help to distinguish between different models and reaction mechanisms for such inclusive reactions.

We have measured  $\alpha$ - and  $^3\text{He}$ -spectra induced by 72 MeV polarized protons on the target nuclei  $^{12}\text{C}$ ,  $^{27}\text{Al}$ ,  $^{58}\text{Ni}$ ,  $^{90}\text{Zr}$  and  $^{209}\text{Bi}$ .

From these spectra, taken in a broad energy range at up to 14 reaction angles, the differential cross section and the angular distribution of analyzing power were extracted.

---

\* Institut für Physik der Universität Basel

We have also measured, using unpolarized protons of 72 MeV, the angular distribution of  $\alpha$ - and  $\tau$ -particles as well as the angle-integrated (p, $\alpha$ x)-cross section for the following target nuclei:  $^{27}\text{Al}$ ,  $^{59}\text{Co}$ ,  $^{90}\text{Zr}$ ,  $^{197}\text{Au}$ ,  $^{208}\text{Pb}$  and  $^{232}\text{Th}$ . In Fig. 1 the angle-integrated  $\alpha$ -spectra of these nuclei are given as a function of the effective excitation energy of the residual nucleus (real excitation energy minus the pairing energy). The target nuclei are identified by the following symbols: x  $^{27}\text{Al}$ ,  $\bullet$   $^{59}\text{Co}$ ,  $\square$   $^{90}\text{Zr}$ ,  $\Delta$   $^{197}\text{Au}$ ,  $\nabla$   $^{208}\text{Pb}$ , +  $^{232}\text{Th}$ .

Figure 2 shows our angular distributions of high energy  $\alpha$ - and  $\tau$ -particles (same notation). The  $\alpha$ - and  $\tau$ -energies  $E_\alpha$  and  $E_\tau$  have been chosen to correspond to the same excitation  $E^* = 66$  MeV above the Fermi-energy of the composite nucleus. The  $\alpha$ -distributions (a and lower angular scale) are normalized to  $^{27}\text{Al}$ . The  $\tau$ -distributions (b and upper angular scale) are normalized to  $^{90}\text{Zr}$ . The full line represents the theoretical prediction for the  $\alpha$ -particles {1}, {2}. The shape of the  $\alpha$ -angular distributions is practically the same for all nuclei considered, independent of the mass number. The same is true for the  $\tau$ -particles. There exists a striking similarity between the angular distribution of  $\alpha$ - and  $\tau$ -particles. We believe that such a finding will prove very useful for developing a theory of  $\tau$ -emission.

A theoretical analysis of our data in the framework of a multi-step-direct calculation is in progress.

#### References

- {1} E. Gadioli et al.  
Proc. Intern. Conf. on Nucl. Reaction Mechanisms,  
Varenna, Italy, June 1979/Clued, Via Celoria 20, Milan
- {2} R. Wagner et al.  
ibid.



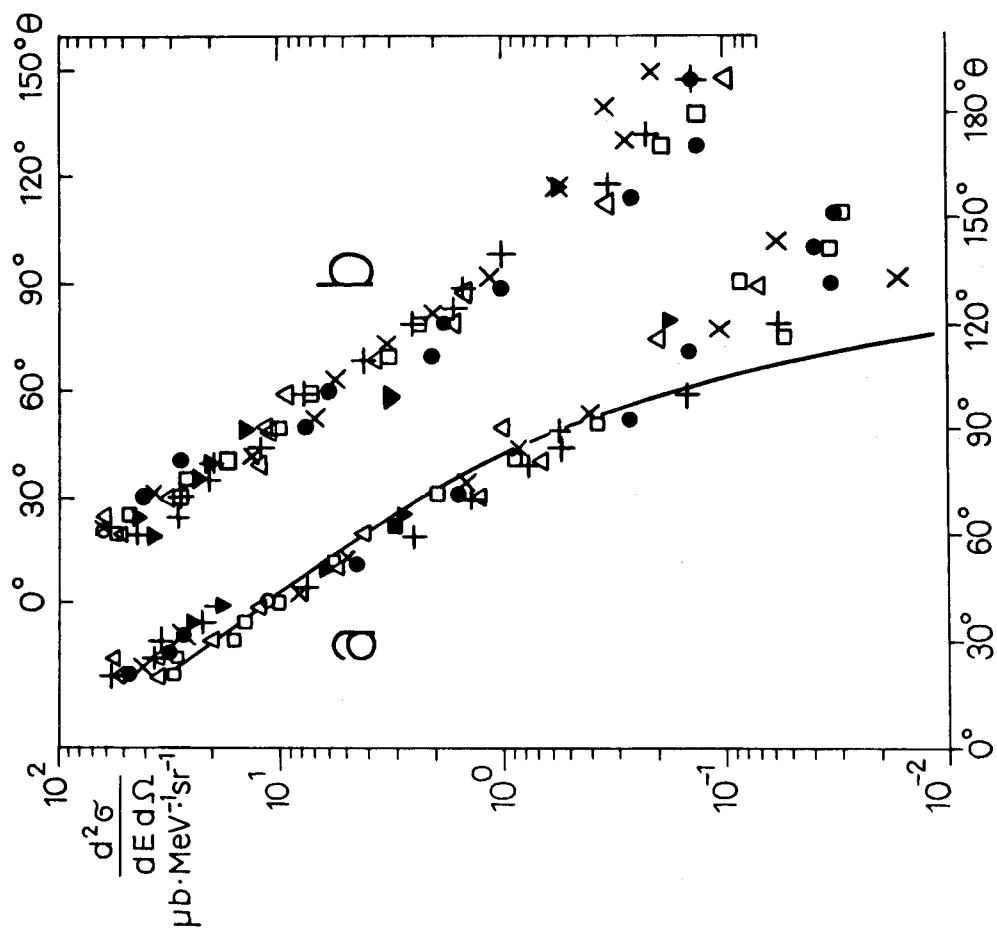
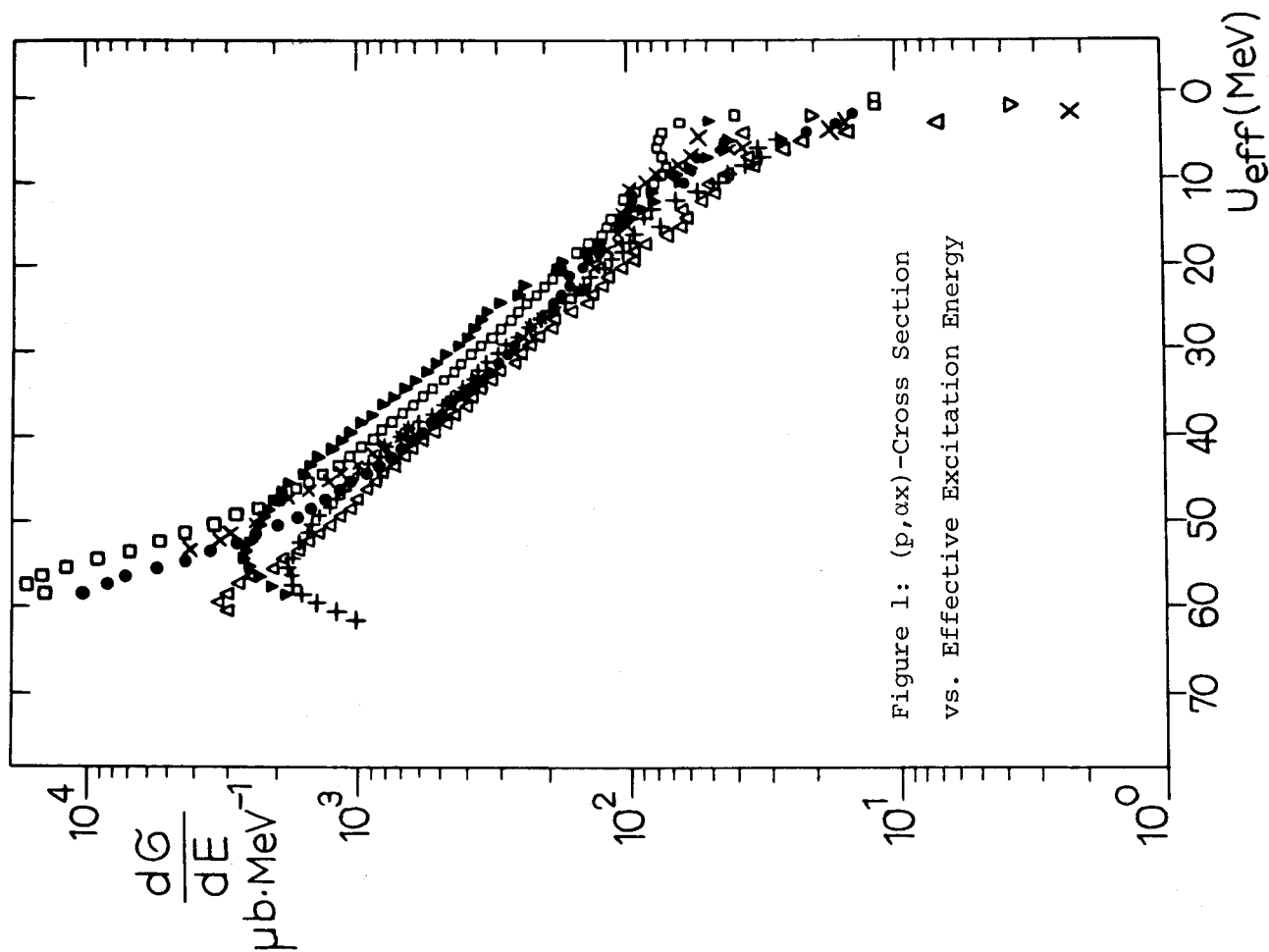


Figure 2: Angular Distributions

at  $E^* = 66 \text{ MeV}$

3. Proton scattering on  $^{64}\text{Zn}$

J. Ramm-Arnet, V. Meyer

Differential cross sections of the reaction  $^{64}\text{Zn}(p,p)^{64}\text{Zn}$  were measured in steps of 0.3 keV to 0.7 keV in the laboratory-energy range from 2.88 MeV to 5.02 MeV at angles of  $90^\circ$ ,  $125^\circ$ ,  $141^\circ$  and  $165^\circ$ . Thereby R-matrix derived parameters of 282 resonances could be determined. By means of the large number of  $1/2^+$ -resonances (227) the distribution of the reduced widths as well as the density distribution of the energy levels and the frequency distribution of the level spacings have also been evaluated. Thus a test of statistical theories is possible.

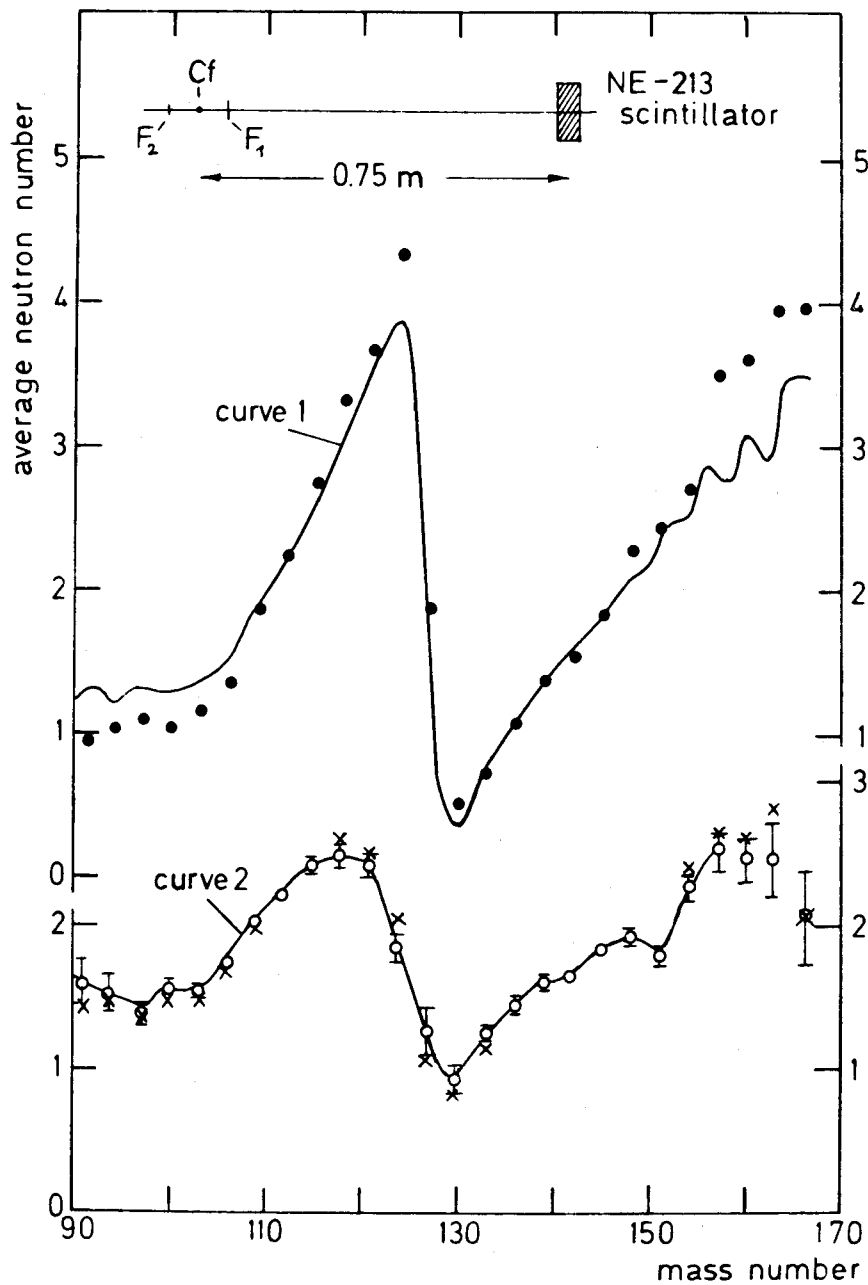
4. Measurement and Analysis of Prompt Fission  
Neutrons of  $^{252}\text{Cf}(\text{sf})$

H.H. Müller et al., P. Riehs\* et al.

Fragments of  $^{252}\text{Cf}(\text{sf})$  have been measured with Si-surface barrier detectors in coincidence with the time of flight of prompt fission neutrons in fragment flight direction. The shape of  $\bar{\nu}(M)$  - the average neutron number as a function of fragment mass - is examined under the assumption that some of the neutron intensity is due to the emission by slowly moving fragments. No remarkable differences are observed between the analysis with and without this assumption. Corrections for the neutron coincidence probability reduce to some extent the pronounced peaks of  $\bar{\nu}(M)$ . Further experiments will be carried out in the near future.

---

\* Atominstitut der Oesterreichischen Universitäten, Wien



Shapes of  $\bar{\nu}(M)$ , the average neutron number as a function of the fragment mass number for  $^{252}\text{Cf}(sf)$ . Curve 1 shows the results from R.L. Walsh and J.W. Boldeman, Nucl. Phys. A276 (1977) 189. The full circles represent our values. Applying corrections for the recoil of the coincident neutron and for the coincidence probability curve 2 is obtained.

III.           Laboratorium für Kernphysik, ETH Zürich

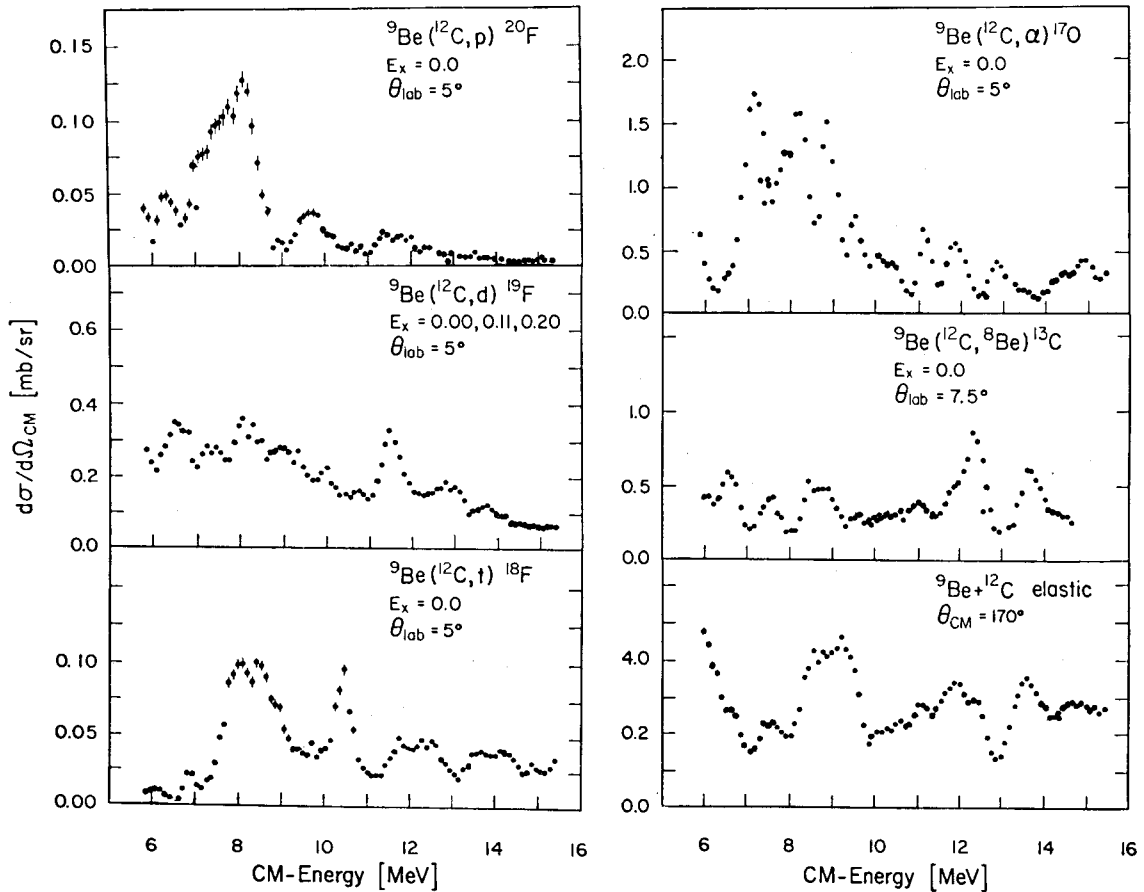
---

1.           Energy dependence of the cross sections in  
              the  $^9\text{Be} + ^{12}\text{C}$  system

M. Hugli et al.

Since the discovery of the resonances in systems as  $^{12}\text{C}+^{12}\text{C}$ ,  $^{12}\text{C}+^{16}\text{O}$  and  $^{16}\text{O}+^{16}\text{O}$  the search for non-statistical structures in the cross sections of heavy ion reactions is an intensively promoted field of nuclear physics. Especially in the system  $^9\text{Be}+^{12}\text{C}$  different authors claim to have demonstrated the existence of many resonances in the energy range between 5 and 15 MeV in the CM system.

With the present work we greatly extend the experimental material and we perform a systematic and critical statistical analysis of all measured excitation curves for the  $^9\text{Be}+^{12}\text{C}$  system. The experiments were performed with the tandem Van de Graaff accelerator of the ETH Zürich. Totally more than 200 excitation curves were measured over an energy range between 6.0 to 15.4 MeV (CM) in steps of 107 keV (CM). The reactions under investigation included the emission of protons, deuterons, tritons, alpha particles and  $^8\text{Be}$  to different states of residual nuclei as well as the elastic scattering. Cross sections were measured for scattering angles in the forward and the backward hemisphere. In the figure a few examples of the measured cross sections are shown. All of them exhibit a pronounced energy dependence. The knowledge of the reliable compound nucleus cross sections and the direct reaction contribution to the different exit channels is the base of each statistical investigation. For this reason angular distributions of the cross sections were measured at six different energies in the range under consideration for several proton, deuteron and alpha channels and a Hauser-Feshbach analysis was performed.



Experimental excitation curves of the  ${}^9\text{Be} + {}^{12}\text{C}$  system for different states or group of states of the residual nucleus

The statistical investigations included the autocorrelation analysis of each excitation curve and the localisation of correlated structure with the aid of different statistical test functions within a set of statistically independent curves. Beside the energy dependent deviation function and cross correlation function the maximum counting method was used. The calculation of the energy average cross correlation coefficients did not point out a strong correlation between some of the curves. Clear evidence for non-statistical phenomena could not be found. Only at the energy of 9.64 MeV (CM) several test functions give a slight indication of an anomalous effect. It is mainly dominated by the alpha channel.

IV. Eidg. Institut für Reaktorforschung, Würenlingen

---

1. Mass distribution in the reactor-neutron  
included fission of  $^{232}\text{Th}$

H.N. Erten, A. Grütter, E. Rössler, H.R. von Gunten

The mass distribution in the reactor-neutron induced fission of  $^{232}\text{Th}$  has been studied using radiochemical techniques and  $\gamma$ -ray spectroscopy. The absolute yields of the standard nuclides  $^{99}\text{Mo}$  and  $^{132}\text{Te}$  were determined by means of an aluminium parallel plate type fission counter. The yields of 36 mass-chains were determined by both, the R-method (relative to  $^{235}\text{U}(n_{\text{th}},f)$ - yields) and the line intensities of selected  $\gamma$ -transitions. The results of both methods are given in Table 1.

The peak-to-valley ratio of the mass-yield curve is found to be about 100. The light and heavy mass peaks are centered at masses 91 and 140 respectively. The results suggest the presence of a small third peak in the valley of the mass distribution.

References

- {1} B.F. Rider, NEDO-12154 (1980).

TABLE I  
Yields in the Fission of  $^{232}\text{Th}$  with Reactor Neutrons

Nuclide	Number of Determinations	R	$^{235}\text{U}$ ( $n_{\text{th}}, f$ )	$^{232}\text{Th}$ ( $n_f, t$ )	Absolute Yields	
			Yields (Ref. 1)	Yields (R-Method)	$^{235}\text{U}$ ( $n, f$ )	$^{232}\text{Th}$ ( $n_f, f$ )
$^{77g}\text{Ge}$ <sup>a</sup>	4	-	-	-	-	0.0113±0.0017
$^{78}\text{Ge}$ <sup>a</sup>	4	-	-	-	-	0.073 ±0.011
$^{83}\text{Br}$	3	8.09±0.61	0.536±0.011	2.13±0.20	0.617	2.42
$^{84}\text{Br}$	3	8.19±0.64	0.956±0.013	3.84±0.31	1.01	3.99
$^{89}\text{Sr}$ <sup>b</sup>	5	3.17±0.15	4.82±0.07	7.50±0.54	-	-
$^{90}\text{Sr}$ <sup>b</sup>	2	2.90±0.23	5.77±0.08	8.21±0.79	-	-
$^{91}\text{Sr}$	3	2.61±0.03	5.93±0.08	7.59±0.42	6.04	7.68
$^{92}\text{Sr}$	3	2.35±0.05	5.90±0.12	6.80±0.41	5.58	6.40
$^{93}\text{Y}$	2	2.16±0.03	6.38±0.38	6.76±0.54	6.18	6.51
$^{95}\text{Zr}$ <sup>c</sup>	2	1.76±0.02	6.52±0.09	5.63±0.31	6.15	5.79
$^{97}\text{Zr}$ <sup>c</sup>	2	1.55±0.08	5.92±0.17	4.50±0.35	5.35	4.01
$^{99}\text{Mo}$	21	1.00	6.07±0.09	2.98±0.15	6.07	2.98
$^{103}\text{Ru}$	4	0.106±0.002	3.03±0.04	0.158±0.009	3.16	0.149
$^{105}\text{Ru}$	4	0.118±0.002	0.969±0.058	0.0561±0.0046	0.952	0.0556
$^{106}\text{Ru}$ <sup>b</sup>	3	0.247±0.040	0.402±0.006	0.0487±0.0085	-	-
$^{109}\text{Pd}$	5	3.48±0.08	0.0330±0.0053	0.0563±0.0096	0.0238	0.0423
$^{111}\text{Ag}$	5	7.50±0.15	0.0191±0.0011	0.0703±0.0056	0.0175	0.0661
$^{112}\text{Pd}$	5	12.13±0.19	0.0130±0.0008	0.0774±0.0042	0.0121	0.0759
$^{113g}\text{Ag}$	5	11.68±0.35	0.0137±0.0011	0.0785±0.0079	0.0160	0.0785
$^{115g}\text{Cd}$	5	11.21±0.11	0.0092±0.0010	0.0506±0.0061	0.0110	0.0578
$^{117m}\text{Cd}$	5	10.30±0.46	0.0045±0.0010	0.0227±0.0053	0.00255	0.0135
$^{117g}\text{Cd}$	5	12.97±0.20	0.0078±0.0018	0.050±0.012	0.00764	0.0408
$^{117m+g}\text{Cd}$	5	12.36±0.20	0.0123±0.0028	0.075±0.017	0.0102	0.0543
$^{127}\text{Sb}$	4	1.32±0.02	0.125±0.010	0.0809±0.0078	0.132	0.0841
$^{129}\text{Sb}$	4	0.843±0.008	0.749±0.045	0.310±0.025	0.717	0.293
$^{131}\text{I}$	3	1.27±0.02	2.89±0.03	1.80±0.10	2.56	1.70
$^{132}\text{Te}$	13	1.50±0.02	4.30±0.04	3.16±0.17	4.22	2.94
$^{134g}\text{I}$	3	1.63±0.07	7.79±0.47	6.23±0.56	6.60	5.27
$^{135}\text{I}$	3	1.99±0.03	6.29±0.13	6.14±0.36	5.50	5.64
$^{139}\text{Ba}$	3	2.28±0.05	6.36±0.09	7.11±0.42	8.22	9.14
$^{140}\text{Ba}$	3	2.67±0.03	6.20±0.09	8.12 ±0.45	6.18	8.02

(continued)

TABLE I (continued)

Nuclide	Number of Determinations	R	$^{235}\text{U}$ ( $n_{\text{th}}, f$ ) Yields (Ref. 1)	$^{232}\text{Th}$ ( $n_f, f$ ) Yields (R-Method)	Absolute Yields	
					$^{235}\text{U}$ ( $n, f$ )	$^{232}\text{Th}$ ( $n_f, f$ )
$^{141}\text{Ce}$	4	$2.59 \pm 0.09$	$5.79 \pm 0.06$	$7.36 \pm 0.47$	5.99	7.58
$^{143}\text{Ce}$	4	$2.38 \pm 0.09$	$5.96 \pm 0.08$	$6.96 \pm 0.46$	5.78	6.73
$^{144}\text{Ce}$	4	$2.96 \pm 0.09$	$5.49 \pm 0.05$	$7.79 \pm 0.49$	5.51	8.02
$^{147}\text{Nd}$	4	$2.74 \pm 0.11$	$2.27 \pm 0.02$	$3.05 \pm 0.20$	2.10	2.68
$^{149}\text{Pm}$	4	$2.18 \pm 0.06$	$1.08 \pm 0.04$	$1.16 \pm 0.08$	1.17	1.20
$^{151}\text{Pm}$	4	$1.92 \pm 0.10$	$0.420 \pm 0.008$	$0.396 \pm 0.030$	0.367	0.317
$^{153}\text{Sm}$	3	$1.33 \pm 0.13$	$0.162 \pm 0.006$	$0.106 \pm 0.012$	0.167	0.104

<sup>a</sup> Values based on the R-method are omitted since the results for  $^{235}\text{U}$  scatter considerably.

<sup>b</sup> Determined by  $\beta$ -counting

<sup>c</sup> Determined by direct  $\gamma$ -ray spectroscopy.

## 2. Radiation damage in fusion first wall materials

U. Stiefel

In continuing the investigation of radiation damages in fusion first wall materials by means of the proton-irradiation experiment (PIREX) at the accelerator of the Swiss Institute for Nuclear Research (SIN) first results have been obtained.

The NMTC (nucleon-meson-transport-code) was used to calculate the nuclear effects that produce the displacement cascades and impurities. The calculations have showed that the displacement damage rate at the SIN accelerator is a few times faster than the damage rate will be in a fusion reactor first wall at the typical wall loading of  $1 \text{ MW/m}^2$ , and the helium production is about 10 times faster. The computer calculations have now completed the case for the SIN accelerator and the



800 MeV case as with the LAMPF proton accelerator in the USA.

A series of irradiations have been made on high purity reference aluminium at  $120^{\circ}\text{C}$  ( $= 0.4 T_m$  where  $T_m$  is the melting temperature). The microstructural response is modified by the helium generation: the usual void structures are still present, but with different distributions than those developed by fission reactor neutrons. A small new feature, helium bubbles we think, are present at and near the grain boundaries in a band where no damage is normally observed. These new defects will very likely affect ductility, creep and fatigue life, electrical and thermal conductivity, just to name some important properties. The highest fluence irradiation so far has produced the same helium content as will be produced at the "end-of-life" in fusion reactors. The microstructural examinations have been conducted principally at RISØ in Denmark, but also with the high voltage electron microscope at Harwell and with microscopes at Cambridge University in England, and with electron microscopes at Los Alamos National Lab., the University of Illinois and Case Western Reserve in the USA.

Continuing irradiations will be made on void resistant alloys (with structures where there is no place for the helium to go but in high pressure bubbles), higher temperatures where the helium bubble effects should be even more severe, and other materials.

#### References

- {1} U. Stiefel, NEANDC (OR) - 154/L, INDC (SWT) - 14/L (1980)